A&A 394, 617–624 (2002)
DOI: 10.1051/0004-6361:20021162

Astronomy & Astrophysics

UBVJHKLM photometry and modeling of R Coronae Borealis⋆

B. F. Yudin[1,2,3], J. D. Fernie[4], N. R. Ikhsanov[2,5], V. I. Shenavrin[1], and G. Weigelt[2]

[1] Sternberg Astronomical Institute, Universitetskii prospect 13, 119899 Moscow, Russia
[2] Max-Planck-Institut für Radioastronomie, Auf dem Hügel 69, 53121 Bonn, Germany
[3] Isaac Newton Institute of Chile, Moscow Branch, Russia
[4] David Dunlap Observatory, University of Toronto, Box 360, Richmond Hill, Ontario L4C 4Y6, Canada
[5] Central Astronomical Observatory RAS at Pulkovo, Pulkovo 65/1, 196140 St. Petersburg, Russia

Received 26 April 2002 / Accepted 7 August 2002

Abstract. We present the results of *UBVJHKLM* photometry of R CrB spanning the period from 1976 to 2001. Studies of the optical light curve have shown no evidence of any stable harmonics in the variations of the stellar emission. In the *L* band we found semi-regular oscillations with the two main periods of ∼3.3 yr and ∼11.9 yr and the full amplitude of $\sim 0\overset{\mathrm{m}}{.}8$ and $\sim 0\overset{\mathrm{m}}{.}6$, respectively. The colors of the warm dust shell (resolved by Ohnaka et al. 2001) are found to be remarkably stable in contrast to its brightness. This indicates that the inner radius is a constant, time-independent characteristic of the dust shell. The observed behavior of the IR light curve is mainly caused by the variation of the optical thickness of the dust shell within the interval $\tau(V) = 0.2{-}0.4$. Anticorrelated changes of the optical brightness (in particular with $P \approx 3.3$ yr) have not been found. Their absence suggests that the stellar wind of R CrB deviates from spherical symmetry. The light curves suggest that the stellar wind is variable. The variability of the stellar wind and the creation of dust clouds may be caused by some kind of activity on the stellar surface. With some time lag, periods of increased mass-loss cause an increase in the dust formation rate at the inner boundary of the extended dust shell and an increase in its IR brightness. We have derived the following parameters of the dust shell (at mean brightness) by radiative transfer modeling: inner dust shell radius $r_{\rm in} \approx 110\,R_*$, temperature $T_{\rm dust}(r_{\rm in}) \approx 860$ K, dust density $\rho_{\rm dust}(r_{\rm in}) \approx 1.1 \times 10^{-20}\,{\rm g\,cm^{-3}}$, optical depth $\tau(V) \approx 0.32$ at 0.55 μm, mean dust formation rate $\dot{M}_{\rm dust} \approx 3.1 \times 10^{-9}\,M_\odot\,{\rm yr^{-1}}$, mass-loss rate $\dot{M}_{\rm gas} \approx 2.1 \times 10^{-7}\,M_\odot\,{\rm yr^{-1}}$, size of the amorphous carbon grains $\lesssim 0.01\,\mu$m, and $B - V \approx -0.28$.

Key words. stars: carbon – stars: circumstellar matter – stars: individual: R CrB – infrared: stars

1. Introduction

R Coronae Borealis is the prototype of a small group of yellow supergiants (about 35 known members in our Galaxy) characterized by sudden declines in their optical brightness and extremely hydrogen-deficient, carbon-rich atmospheres. The visual light curve of R CrB contains quasi-regular low-amplitude variations without any dominating periods. These are commonly interpreted in terms of stellar pulsations and episodic deep declines, which typically last a few months and have amplitudes of up to 8 mag. Such events are thought to be the result of obscuration by dust clouds generated spasmodically and blown away from the star by radiation pressure (Clayton 1996 and references therein).

The near-infrared excess, discovered by Stein et al. (1969), is assigned to a warm dust shell (blackbody temperature of ∼900 K). This extended dust shell was resolved for the first time by speckle interferometric observations with the SAO 6 m telescope (Ohnaka et al. 2001). The IR excess contributes about 30% of the total flux and is permanently present, regardless of the visual brightness of the object. The *L* flux of R CrB, which is mainly due to dust emission, varies semi-regularly with a period of 1260 days (Feast et al. 1997 and references therein). The analysis of IRAS observations at 60 μm and 100 μm (Gillett et al. 1986) led to the discovery of a very extended "fossil" shell around R CrB, whose diameter and temperature are $\simeq 18'$ and 30 K, respectively.

In this paper we focus on the investigation of the time-dependent characteristics of the extended warm dust shell and their interpretation. In the next section we present the results of our photometric observations of R CrB (*UBV* in 1994–1999 and *JHKLM* in 1983–2001) and the complete tables of photometric observations of the star in 1976–2001. The basic characteristics of the optical and IR radiation of the star during its bright state are analyzed in Sect. 3. Radiative transfer modeling of the warm dust shell at its average brightness is described in Sect. 4. The variations of the dust shell brightness and colors, and, correspondingly, its structural parameters, are investigated in Sect. 5. Our results are discussed in Sect. 6.

Send offprint requests to: B. Yudin,
e-mail: yudin@sai.msu.ru

⋆ Tables 1 and 2 are only available in electronic form at the CDS via anonymous ftp to cdsarc.u-strasbg.fr (130.79.128.5) or via http://cdsweb.u-strasbg.fr/cgi-bin/qcat?J/A+A/394/617

2. Observations

Our *UBV* observations of R CrB were carried out in the period 1994–1999 with the 0.25 m telescope of the Fairborn observatory (Genet et al. 1987). The results of these observations together with those of earlier observations (1985–1993) by Fernie & Seager (1994) are summarized in Table 1 in `http://infra.sai.msu.ru/ftp/rcrb`. This table contains 1170 measurements with the accuracy of $0\overset{\mathrm{m}}{.}02$ or better. The standard star was HD 141352: $V = 7.476$, $B - V = 0.439$ and $U - B = -0.003$.

JHKLM observations were carried out between 1983 and 2001 with the 1.25 m telescope of the Crimean Station of the Sternberg Astronomical Institute (for technical details see Nadjip et al. 1986). The results our observations, together with those obtained in 1976–1979 (Shenavrin et al. 1979), are summarized in Table 2 in `http://infra.sai.msu.ru/ftp/rcrb`. This table contains 252 measurements with the accuracy of $0\overset{\mathrm{m}}{.}03$ or better. The standard star was BS 5947: $J = 2.09$, $H = 1.60$, $K = 1.30$, $L = 1.12$ and $M = 1.35$.

The *VJKLM* light curves of R CrB during the period 1983–2001 are presented in Fig. 1. Also plotted are a few estimates in the *V* band taken from the internet page of the association of amateur astronomers VSOLJ (`http://www.kusastro.kyoto-u.ac.jp/vsnet`) and the measurements reported by Feast et al. (1997) in the *J* and *L* bands. As one can see in this figure, a number of deep declines of the star's visual brightness were observed in 1983–1989 and 1995–2001, while during the interval 1989–1995 the *V* flux was almost constant. The very different behavior of the *L* and *M* light curves will be discussed in subsequent sections.

3. Basic characteristics of R CrB in the bright state

We call the state of R CrB as bright, if $V \leq 6.05$ and $J \leq 5.25$. In this state the contribution of the dust to the optical radiation of R CrB is negligible. The average *UBVJHKLM* and *RI* magnitudes of R CrB in the bright state are summarized in Table 3. These values were derived from Tables 1 and 2, and the data presented by Fernie (1982) and Fernie et al. (1986). The maximum magnitudes of R CrB during the whole observing period are $V \approx 5.69$ and $J \approx 4.89$.

3.1. Periodicity

The Fourier analysis of the visual light curve (1985–1999) during the bright state has revealed a number of harmonics with the full amplitude of $\sim 0\overset{\mathrm{m}}{.}05$ concentrated in the interval of 30–60 days. The maximum amplitude of $0\overset{\mathrm{m}}{.}07$ has the mode with the period $P \approx 39.8$ days (see Fig. 2). The corresponding harmonic with the full amplitude of $\sim 0\overset{\mathrm{m}}{.}025$ was also found from the analysis of the $B - V$ curve. The brightness maxima follow the color minima with a lag of 3 days, and the ratio of the amplitudes of $(B - V)$ and *V* harmonics is about 0.3. No trend has been found in the optical brightness. It should be noted that on a time-scale of several hundreds of days R CrB can occasionally exhibit well-developed pulsations with periods of 35, 44 and 51 days (Fernie & Seager 1994 and references therein).

Table 3. The average magnitudes of R CrB in bright state. $< m >$, $< m >_{L,\max}$, and $< m >_{L,\min}$ denote the magnitudes during the average, maximum and minimum star brightness in the *L* band

Bands	$< m >$	$< m >_{L,\max}$	$< m >_{L,\min}$
U	6.55	6.38	6.82
B	6.49	6.35	6.70
V	5.91	5.81	6.08
R	5.49	5.40	5.62
I	5.31	5.23	5.40
J	5.08	5.01	5.11
H	4.91	4.76	5.08
K	4.13	3.74	4.56
L	2.38	1.79	3.12
M	1.70	0.97	2.48

The low-amplitude quasi-regular variability in the *J* band resembles that in the optical region. A period search has revealed three main harmonics with periods of 43.7, 33.2, and 28.1 days and an amplitude of about $0\overset{\mathrm{m}}{.}08$. At the same time Rao et al. (1999) have found that the radial velocity curve exhibits the only one stable pulsation period of about 42.7 days.

3.2. Spectral energy distribution

The spectral energy distribution (SED) of R CrB relating to its average brightness in bright state (see Table 3) is shown in Fig. 3.

The stellar magnitudes were corrected for the interstellar reddening according to the color excess $E(B - V) = 0.05$ (Asplund et al. 1997). The flux at 0.23 and 0.25 μm was measured with IUE on 31.05.1991 (see INES data from the IUE satellite), when the star brightness in the visual and near IR was close to its average values in bright state presented in Table 3.

To reconstruct the SED beyond 10 μm we used observation of R CrB with IRAS on 12-13.09.1983 (Rao & Nandy 1986). The *L* flux of the star on these dates was smaller than its average value ($\Delta L \simeq 0.25$). To account for this difference the fluxes measured by IRAS at 12, 25, 60 and 100 μm were increased by 8%, taking into account that $\Delta f(3.5\ \mu\mathrm{m})/\Delta f(11\ \mu\mathrm{m}) \approx 3$ (Forrest et al. 1972).

Integrating the SED presented in Fig. 3 we evaluate the average bolometric flux of R CrB during its bright state as $F_{\mathrm{bol,mean}} \approx 1.55 \times 10^{-7}$ erg cm^{-2} s^{-1}. About 85% of the radiation detected from the star is emitted within the interval 0.36 μm $\lesssim \lambda \lesssim$ 5 μm, which is completely covered by our photometric observations. The contributions at $\lambda \lesssim 0.36$ μm, $\lambda \gtrsim 5$ μm and $\lambda \gtrsim 12$ μm are 4%, 10% and 3%, respectively. In particular, this indicates that the possible errors in the correction of the IRAS data cannot significantly change the estimates of the bolometric flux.

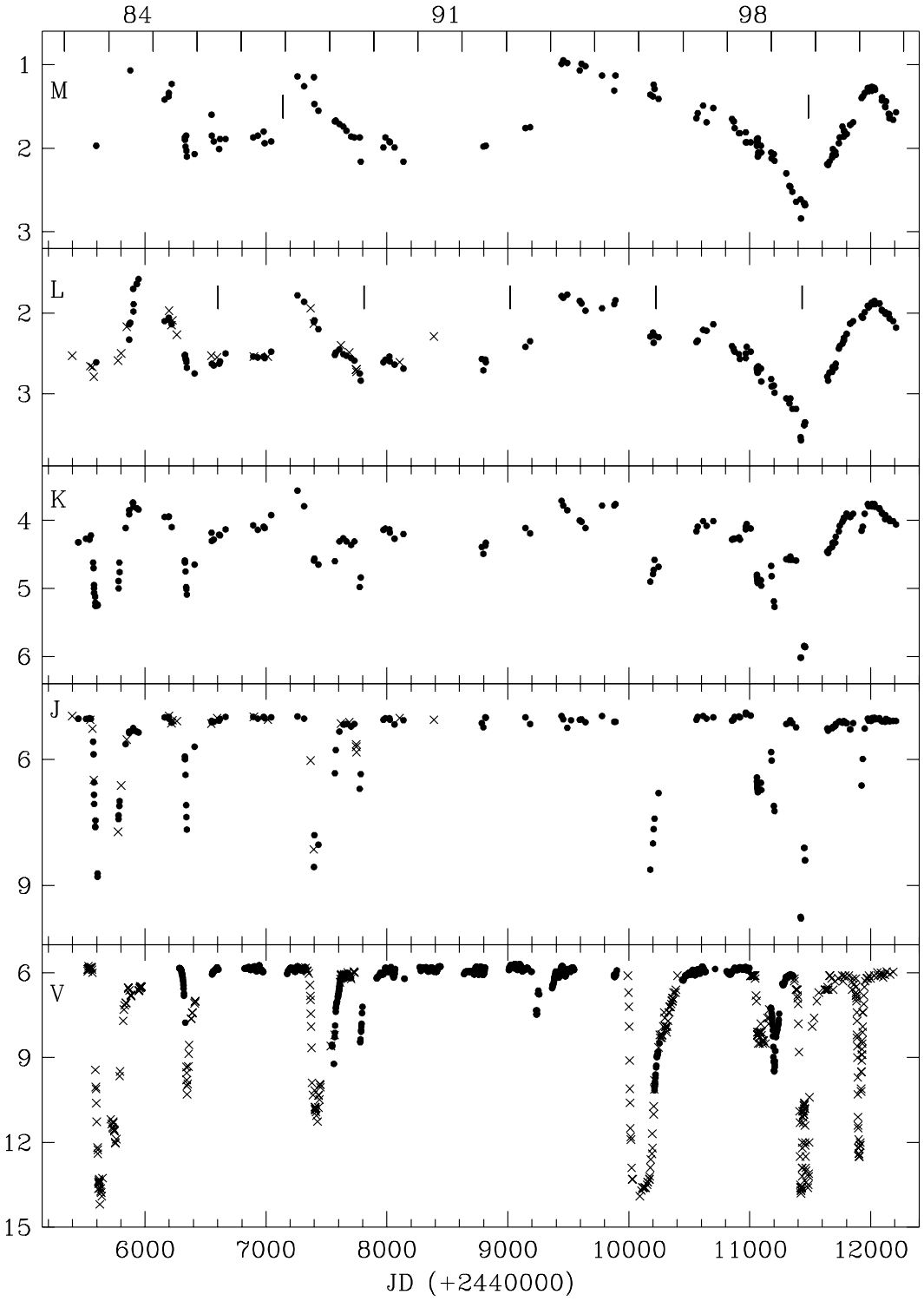

Fig. 1. *VJKLM* light curves of R CrB. The dots represent the observations reported in this paper. The crosses in the visual light curve denote the data of VSOLJ (`http://www.kusastro.kyoto-u.ac.jp/vsnet`), and in the *J* and *L* light curves, the data reported by Feast et al. (1997). The vertical bars in the *L* and *M* panels mark the times of the minima calculated from Eqs. (14) and (15), respectively.

3.3. Infrared excess

The strong infrared excess (i.e. the bolometric flux of the dust shell) can be evaluated as $F_{\rm dust} = F_{\rm bol} - F_{*,\rm bol}$. Here $F_{\rm bol}$ is the observed bolometric flux and $F_{*,\rm bol}$ is the bolometric flux emitted by the central star and passed through the dust shell.

To evaluate the infrared excess we have to reconstruct the observed SED of the star ($F_*(\lambda)$). The upper limit of the contribution of the dust shell in the *J* band can be derived directly from our observations in 1996. In this year a deep decline was observed ($\Delta J \geq 3.6$), while its *L* brightness was close to the average value presented in Table 3. Attributing the observed

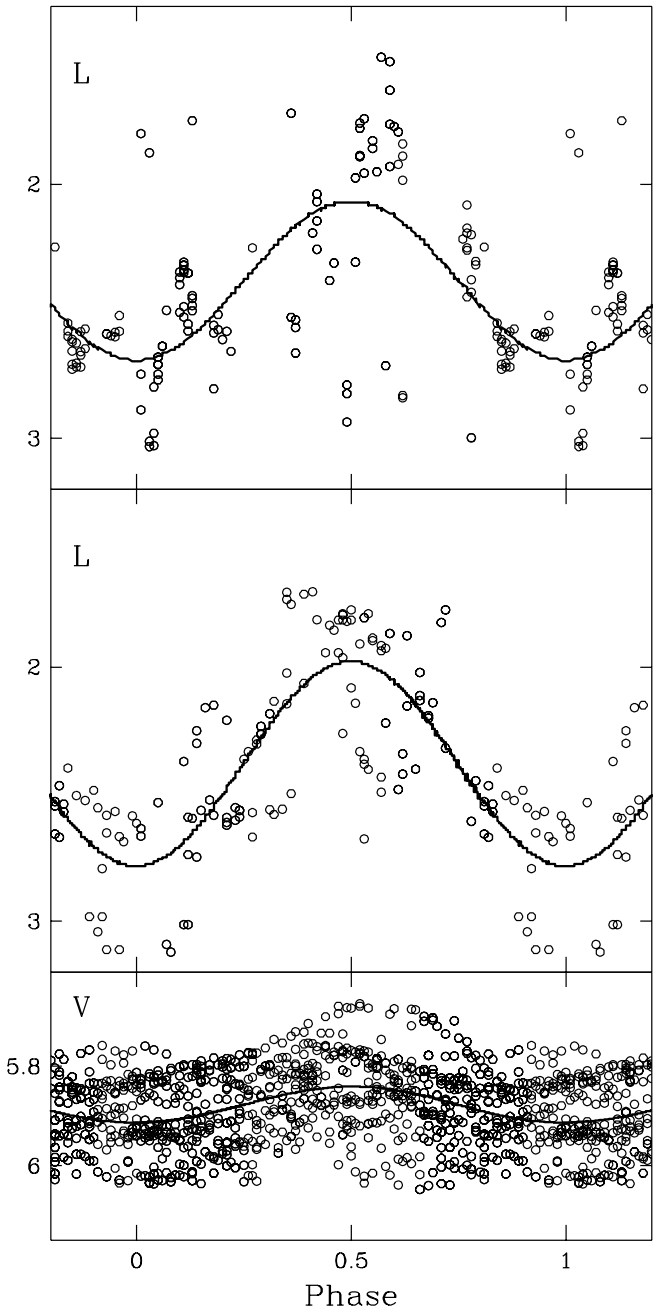

Fig. 2. The V and L light curves of R CrB folded with the periods 39.82, 1206 and 4342 days, from bottom to top.

J flux in minimum to the dust shell we conclude that its contribution to the total flux out of minimum is smaller than 4%. This indicates that within the interval $\lambda \leq 1.25$ μm the total flux is approximately equal to $F_*(\lambda)$.

To evaluate $F_*(\lambda)$ in *HKLM* we use the intrinsic colors of R CrB stars calculated by Asplund et al. (1997). They depend on the effective temperature and the gravitational acceleration on the star surface. For R CrB we take $T_{\rm eff} \approx 6750$ K, $L_{\rm bol} \approx 10^4\ L_\odot$, $\log g \approx 0.5$, radius $R_* \approx 73.4\ R_\odot$, and correspondingly the intrinsic colors $(H-K)_0 \approx 0.07$, $(K-L)_0 \approx 0.06$ and $(L-M)_0 \approx 0.03$ (Asplund et al. 1997; Asplund 2000). These colors were corrected for the interstellar and circumstellar reddening although both of these corrections have only

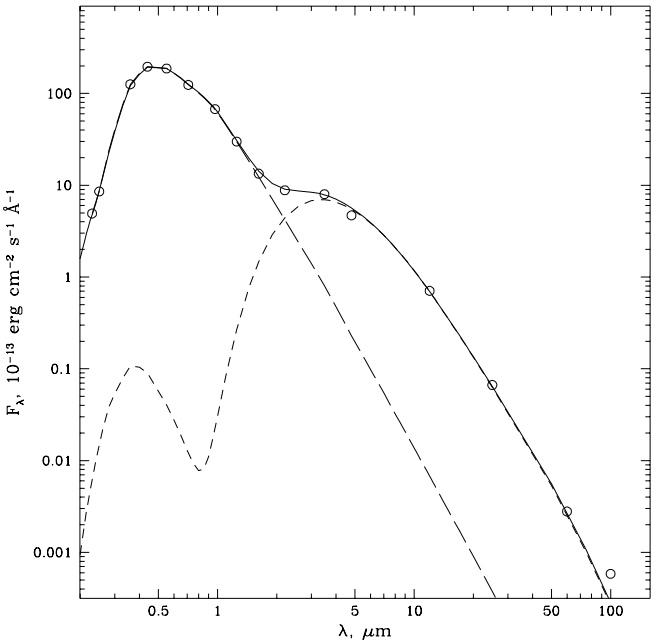

Fig. 3. SED of R CrB for average brightness in bright state (circles). Long- and short-dashed lines denote the SED of the star and the dust shell, respectively. The solid line is the fitted SED (see text).

a minor effect on the evaluation of $F_{*,\rm bol}$. For $\lambda \geq 4.8$ μm we approximate $F_*(\lambda)$ by the blackbody spectrum with the effective temperature 6750 K.

The derived SED of the star is presented in Fig. 3 (long-dashed line). Integrating $F_*(\lambda)$ we find $F_{*,\rm bol} \approx 1.17 \times 10^{-7}$ erg cm^{-2} s^{-1} and $F_{\rm dust,mean} \approx 3.8 \times 10^{-8}$ erg cm^{-2} s^{-1}. This means that about 24% of the stellar radiation is absorbed and re-emitted by the dust shell. Assuming the geometry of the dust shell to be spherically symmetric, one can estimate its optical depth as $\tau_{\rm eff,mean} \approx 0.28$. For yellow stars and amorphous carbon grains the value of the $\tau_{\rm eff,mean}$ differs from the optical thickness at 0.55 μm (τ(V)) by a few percent.

3.4. Color–brightness diagrams of the star

The derived color–brightness diagrams $(U-B, V)$, $(B-V, V)$, $(V-R, V)$, $(V-I, V)$ and $(V-J, V)$ are presented in Fig. 4. These diagrams have been constructed using the data from Tables 1 and 2 and the values reported by Fernie (1982) and Fernie et al. (1986). For the diagram $(V-J, V)$ we have chosen the estimates which were obtained in all three bands on the same date. Only the data relating to the star brightness in the L band smaller than the average value were used. The J flux has been reduced by 4% in order to exclude the contribution of the dust shell. The linear approximation of the diagrams yields

$$U - B = 0.402V - 2.31, \quad (1)$$

$$B - V = 0.280V - 1.08, \quad (2)$$

$$V - R = 0.301V - 1.36, \quad (3)$$

$$V - I = 0.430V - 1.94, \quad (4)$$

$$V - J = 0.418V - 1.62. \quad (5)$$

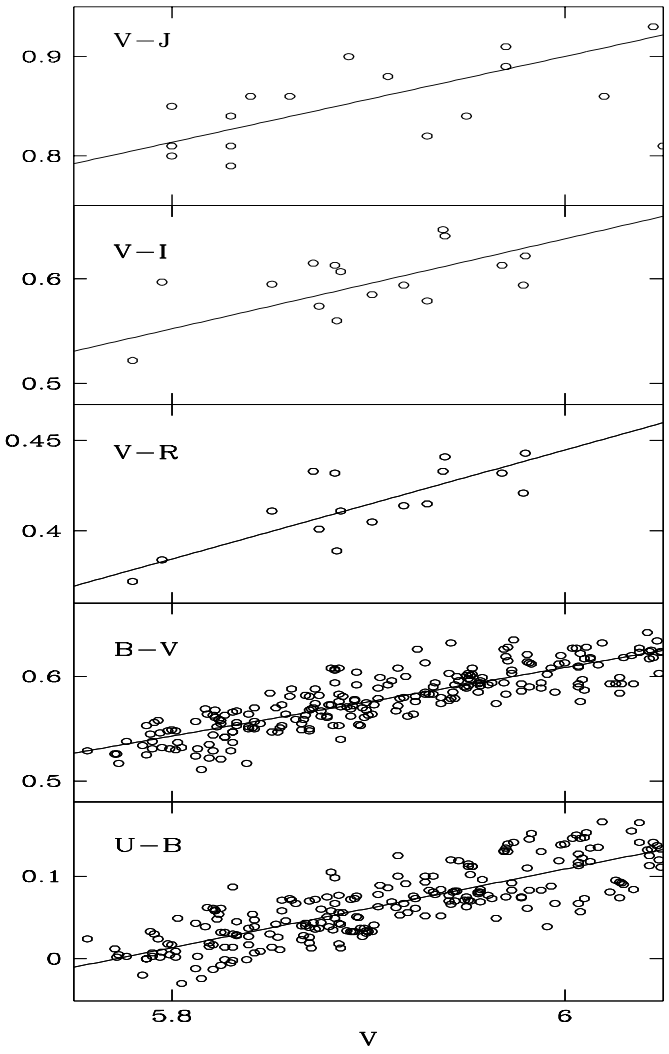

Fig. 4. $(U-B, V)$, $(B-V, V)$, $(V-R, V)$, $(V-I, V)$ and $(V-J, V)$ diagrams. The solid lines denote the approximations by linear Eqs. (1)–(5).

where $5.79 \leq V \leq 6.05$. It follows from these equations that the star reddens as its light declines.

4. Modeling of the warm dust shell at its mean brightness in bright state

Using the quasi-diffusion method of Leung (1976), as implemented in the CSDUST3 code (Egan et al. 1988), we have constructed radiative transfer models which match the SED of R CrB. The input parameters of the models were the same as described by Yudin et al. (2001).

As a first approximation we have assumed that the warm dust shell is spherical and consists of amorphous carbon grains with the radius $a_{\rm gr} = 0.01$ μm. The efficiencies of absorption and scattering of the dust grains were calculated using the Mie theory. The refractive index was taken from Jäger et al. (1998, sample cel1000). The intrinsic SED of the star emission, $F_{*,0}(\lambda)$, was calculated as $F_{*,0}(\lambda) = F_*(\lambda)e^{\tau(\lambda)}$, where $\tau(\lambda)$ is the total optical depth at a given reference wavelength. The reference wavelength was chosen to be 0.55 μm, and the model SED is normalized to the observed one in the V band.

We have derived the following parameters of the dust shell which refer to its mean brightness in bright state. The optical depth at 0.55 μm and 2.2 μm are $\tau(V) \approx 0.32$ and $\tau(K) \approx 0.05$, respectively. The inner radius of the dust shell is $r_{\rm in} \approx 110\,R_*$. The temperature and the dust density at the inner radius of the dust shell are $T_{\rm dust}(r_{\rm in}) \approx 860$ K and $\rho_{\rm dust}(r_{\rm in}) \approx 1.1 \times 10^{-20}$ g cm^{-3}, respectively, and the density distribution of the dust shell is $\rho(r) \propto r^{-2}$.

Using these parameters we have evaluated the dust formation rate at the inner boundary of the dust shell as $\dot{M}_{\rm dust} \approx 3.1 \times 10^{-9}\ M_\odot$ yr^{-1}. If one assumes that almost all carbon is bound in the dust grains and uses the chemical composition of the atmosphere of R CrB from Asplund et al. (2000), the gas density at the inner radius of the dust shell is $\rho_{\rm gas}(r_{\rm in}) \approx 7.3 \times 10^{-19}$ g cm^{-3}. Correspondingly, with a stellar wind velocity of $V_{\rm env} \approx 45$ km s^{-1}, which is typical for stars of this type, one finds a mass outflow rate in R CrB of $\dot{M}_{\rm gas} \approx 2.1 \times 10^{-7}\ M_\odot$ yr^{-1}. If, however, a fraction of the carbon and almost all of the oxygen are bound in the CO molecule, the corresponding estimates of $\rho_{\rm gas}(r_{\rm in})$ and $\dot{M}_{\rm gas}$ turn out to be larger by a factor of 2.5.

As follows from our modeling, the visual brightness of the dust shell is $V \approx 14\overset{\rm m}{.}6$ and its color indices are $U-B \approx -0.65$, $B-V \approx -0.28$, $V-R \approx -0.41$ and $R-I \approx 1.47$. The SED of the dust shell is plotted in Fig. 3 (short-dashed line). The radiation of the dust shell in *UBVR* is dominated by scattering. Since the radius of the grains is significantly smaller than the wavelength, the scattering is governed by the Rayleigh law ($\sigma_{\rm sca} \propto \lambda^{-4}$). This explains the blue colors of the dust shell in this part of the spectrum. In the I band the thermal emission of the grains begins to dominate over the scattering.

The visual magnitude of R CrB observed during the deepest declines is about $14^{\rm m}$. Thus, the visual magnitude of the dust shell should be fainter than $14^{\rm m}$. This was the reason for choosing a small radius of the dust grains ($\sim$0.01 μm) in our calculations. If one assumes that the radius of the dust grains is larger, the visual brightness of the dust shell becomes greater than that of the star brightness in deep minima. For instance, increasing the radius of the dust grains by a factor of 2.5 (i.e. to 0.025 μm), one finds a visual magnitude of the dust shell of $V \approx 11\overset{\rm m}{.}5$. This reflects the fact that the albedo of dust grains rapidly increases with their radius.

We have also found the colors of the dust shell to be sensitive to the value of $r_{\rm in}$. Variations of this parameter of only 10% lead to variations of the IR excess color indices $(H-K)_{\rm dust}$ and $(K-L)_{\rm dust}$ by $\sim 0\overset{\rm m}{.}1$. At the same time these indices are observed to be remarkably stable in contrast to the brightness of the dust shell (see Sect. 5). In the context of our model this means that the value of the inner radius $r_{\rm in}$ is a fairly constant, time-independent characteristic of the extended warm dust shell. It should be noted, however, that the absolute value of $r_{\rm in}$ depends on the optical properties of the dust grains included in the model calculations. If we used the extinction of amorphous carbon obtained by Colangeli et al. (1995) (ACAR sample) instead of cel1000 (Jäger et al. 1998), the value of $r_{\rm in}$ would be smaller by a factor of $\sim$1.4.

Table 4. The bolometric flux, the infrared excess and the optical thickness of the dust shell of R CrB during maximum and minimum of L brightness.

	$F_{\rm bol}$ erg cm^{-2} s^{-1}	$F_{\rm dust}$ erg cm^{-2} s^{-1}	$\tau_{\rm eff}$
Maximum	1.90×10^{-7}	6.1×10^{-8}	0.39
Minimum	1.24×10^{-7}	2.1×10^{-8}	0.19

Finally, according to Reimers equation (Reimers 1975), the average mass loss by a yellow supergiant can be estimated as

$$\dot{M} = 4 \times 10^{-13}\, \eta\, \frac{L_* R_*}{M_*}\, M_\odot\, {\rm yr}^{-1}, \quad (6)$$

where L_*, R_* and M_* are the luminosity, the radius and the mass of the star expressed in the solar units, and the dimensionless parameter η is limited to $0.3 \le \eta \le 3$. Using the corresponding parameters of R CrB we find $\dot{M} \approx 4.2 \times 10^{-7}\, \eta\, M_\odot$ yr^{-1}. This is in agreement with the mass outflow rate derived from our model provided $\eta \approx 0.5$. Therefore, the mass loss rate of R CrB agrees with the Reimers equation and no superwind is required for the interpretation of the dust shell formation.

The large value of $r_{\rm in} \approx 110\, R_*$, which does not change significantly with time, suggests that the extended warm dust shell of R CrB originates in a similar way as in the case of ordinary supergiants, i.e. it is caused by the stellar wind and at a large distance from the star. In addition to this common type of dust shell of supergiants, the circumstellar shell of R CrB contains dust clouds which condense somewhere in the vicinity of the star from high density gas clumps (Feast 1997). These additional dust clouds can explain the deep minima in the visual light curve. If the dust clouds are considered as an additional source of the IR emission, then the effective size of this source is much smaller then the size of the above extended dust shell, which condenses from the stellar wind. Until now all efforts to pick out the emission of this consortium of the dust clouds from the total IR excess were unsuccessful (Feast 1997).

5. Variability of the warm dust shell

5.1. The dust shell during maximum and minimum brightness

The *UBVRIJHKLM* magnitudes of R CrB during its maximum (in 1994 April–May) and minimum (in 1999 May–June) brightness in L are presented in the second and third columns of Table 3, respectively. The corresponding bolometric flux and infrared excess of R CrB, and the optical thickness of the dust shell derived using these data are presented in Table 4.

As follows from Table 4, the amplitude of variations of the optical thickness of the dust shell in R CrB is $\Delta\tau \approx 0.2$. At the same time, the value of the color index $(K-L)_{\rm dust}$ of the IR excess, estimated during maximum and minimum brightness in the L band, proves to be the same: $(K-L)_{\rm dust} \approx 2\overset{\rm m}{.}35$. This indicates that the variations of the optical depth of the dust shell cannot be explained by the variations of its inner radius, but reflect the changes of the dust formation rate at a certain distance from the star.

5.2. Colors and the optical thickness of the dust shell

Figure 5 shows the color diagrams $(H_{\rm dust}, L_{\rm dust})$, $(K_{\rm dust}, L_{\rm dust})$, and $(M_{\rm dust}, L_{\rm dust})$. The dots in these diagrams denote IR observations of R CrB when the star was in its bright state. It was assumed that the contribution of the dust shell to the flux in J band is negligibly small. The stellar magnitudes in $HKLM$ and the infrared excess have been derived using the method described above. The linear approximation of the diagrams gives

$$H_{\rm dust} = 1.22 L_{\rm dust} + 4.22, \quad (7)$$

$$K_{\rm dust} = 0.97 L_{\rm dust} + 2.35, \quad (8)$$

$$M_{\rm dust} = 0.98 L_{\rm dust} - 0.66. \quad (9)$$

For the mean L brightness, $L_{\rm dust,mean} \approx 2.49$, we find $(H-L)_{\rm dust,mean} = 4.76 \pm 0.4$, $(K-L)_{\rm dust,mean} = 2.28 \pm 0.15$, and $(L-M)_{\rm dust,mean} = 0.70 \pm 0.12$.

As follows from Eqs. (7)–(9), the variations of the dust shell brightness are not accompanied by remarkable variations of its colors. Hence, there is a proportionality between the bolometric stellar magnitude of the dust shell, $m_{\rm dust,bol}$, and its L magnitude:

$$m_{\rm dust,bol} \simeq L_{\rm dust} + 4\overset{\rm m}{.}55. \quad (10)$$

We can calculate the function $\tau_{\rm eff} = f(F_{\rm dust})$ from the expression $F_{\rm dust} = F_{\rm bol}(1-\exp(-\tau_{\rm eff}))$. Finally, using a quadratic polynomial approximation of the functions $L_{\rm dust} = f(L)$ for the data of our IR observations, we find:

$$m_{\rm dust,bol} \simeq 0.046 L^2 + 0.88 L + 4.68, \quad (11)$$

$$\tau_{\rm eff} \simeq 0.176 L^2 - 1.20 L + 2.14. \quad (12)$$

The function $\tau_{\rm eff}(t)$ for the period 1994–2001 is plotted in Fig. 6. Our modeling has shown that such a sharp transition from the decrease to the increase of the optical depth requires an abrupt change of the dust formation rate close to the minimum. This means that there was a sharp density enhancement in the stellar wind. The solid line in Fig. 6 shows the function $\tau_{\rm eff}(t)$, calculated with the assumption that at minimum the rate of dust formation sharply increases in the minimum of $\tau_{\rm eff}$ by a factor of 4.3, and then rises $\propto t^{1.3}$ during about 560 days until the maximum value of the optical depth is reached.

The dust formation rate depends on the gas density at the inner boundary of the dust shell and, therefore, on the intensity of the mass-loss. The time lag between the increase of the stellar wind and the increase of gas density at the inner radius of the shell is

$$t_{\rm lag} = \frac{r_{\rm in}}{V_{\rm env}} \simeq 4 \left(\frac{r_{\rm in}}{110\, R_*}\right) \left(\frac{V_{\rm sw}}{45\ {\rm km\ s^{-1}}}\right) {\rm yr}. \quad (13)$$

Interestingly, this 4-year wind travel time can probably be seen in the V and L light curves. The comparison of the V and L light curves shows that the period 1994–1999 of decreasing L and M brightness follows approximately 4 years after the period of constant V magnitude between 1989 and 1995. We suggest the following explanation for this. We assume that during phases of increased stellar activity there is a simultaneous

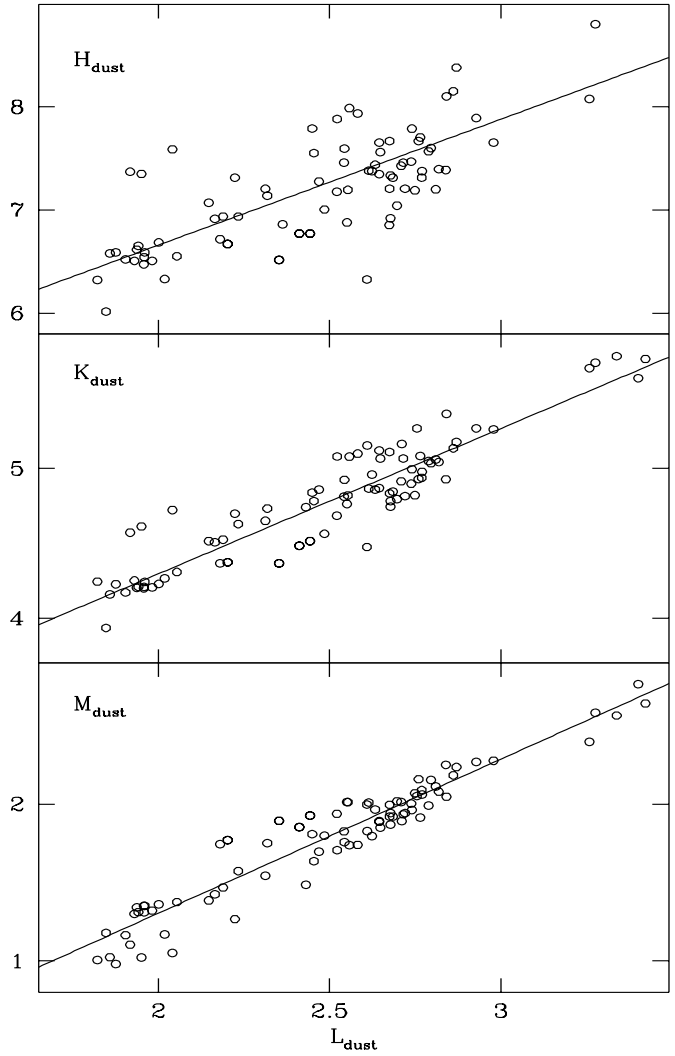

Fig. 5. The ($H_{\rm dust}$, $L_{\rm dust}$), ($K_{\rm dust}$, $L_{\rm dust}$) and ($M_{\rm dust}$, $L_{\rm dust}$) diagrams of the emission of the dust shell. The solid lines denote the approximations by linear Eqs. (7)–(9).

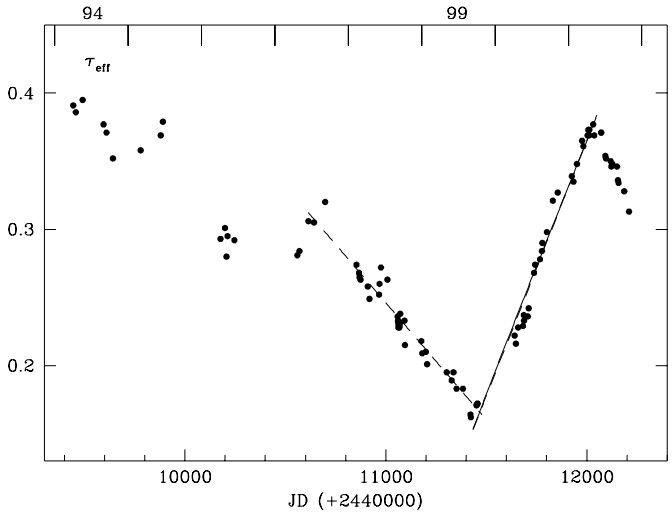

Fig. 6. Optical thickness $\tau_{\rm eff}$ of the dust shell versus time (see text).

increase of both (1) the stellar (supergiant) wind and (2) the rate of the formation of (eclipsing) dust clouds (and we assume that the eclipsing dust clouds cause the deep minima in the V light curve). If these two effects are correlated, then 1983–1989 (with several V minima) was a period of increased activity and, therefore, increased stellar wind. After the wind travel time of approximately 4 years, this increased stellar wind arrived at the extended dust shell region and then caused the L band brightness increase. On the other hand, in the period 1993–1999 the L band brightness was decreasing because in this period only lower intensity stellar wind arrived, which was produced during the low-activity period 1989–1995 (high V brightness).

5.3. Periodicity

In order to search for the periodicity in the variations of the dust shell brightness, i.e. of the mass-loss rate, the L light curve has been analyzed using the code developed by Yu. K. Kolpakov (`http://infra.sai.msu.ru/prog/kolpakov`). We combined our observations with the data presented by Strecker (1975; 35 points during 1968–1974) and Feast et al. (1997; 24 points during 1983–1991), and removed the points obtained during visual declines. Two harmonics of semi-regular variations of the star brightness in the L band were derived: $P_1 \simeq 1206$ days, $\Delta L_1 \approx 0\overset{\rm m}{.}8$ and $P_2 \simeq 4342$ days, $\Delta L_2 \approx 0\overset{\rm m}{.}6$. The corresponding phase diagrams are presented in Fig. 2. The dates of minima of these harmonics are given by the following expressions:

$$\min(L_1) = 2442986 + 1206^d\mathrm{E}, \quad (14)$$

$$\min(L_2) = 2442860 + 4342^d\mathrm{E}. \quad (15)$$

These dates are marked by vertical bars in Fig. 1. The minima of these harmonics coincided in 1999, when the star brightness in L and M was in unusually deep minimum. It should be noted that the existence of the two dominant modes superimposed with irregular variations makes the L light curve quite complex. Moreover, the shape of the harmonics differs from the simple sine wave shown in Fig. 2. For example, the rise of the L brightness in 1984 and 1988 was rather sharp compared to the subsequent declines (Fig. 1). The values of the derived periods are very close to those of the mean time interval between the individual visual declines of R CrB, ~1100 days (Jurcsik 1996), and between groups of visual minima, ~4400 days (Rosenbush 2001).

In the bright state of R CrB, the L variability is mainly caused by changes of the optical depth of the shell. Hence, if the dust shell is spherical, we would expect to find the corresponding semi-regular variations in the visual star brightness with period $P_1 \approx 1206$ days, which are anti-phased to those in the L band. According to Eq. (14) their full amplitude would be $\Delta V \approx 0.3$ mag. However, a period search has not revealed this harmonic in the V light curve. This indicates that the density of the stellar wind (and, correspondingly, the shell density) along the line of sight is smaller than the average one, i.e. the dust shell is asymmetric.

In this case the derived optical depth of the dust shell can be considered as the sphere-averaged one. If the dust shell is optically thin, then its bolometric flux is proportional to the optical

depth averaged over the sphere. Since the shell's SED is primarily defined by the value of the inner radius (i.e., $T_{\rm dust}(r_{\rm in})$) our above results concerning the inner radius (its size and time-independence) and mass-loss rate would be valid.

6. Concluding remarks

We have presented optical and IR long-term monitoring and radiative transfer modeling of R CrB. These studies have allowed the derivation of various time-dependent properties of both (i) the star itself at bright state and (ii) an extended dust shell (similar to that observed around many supergiants) which condenses from the supergiant wind at a large distance of approximately 100 stellar radii from the star. This extended dust shell is larger than the suggested region of dust clouds (distance approx. 2–30 stellar radii, see, e.g. Clayton 1996; Fadeyev 1988), which causes the deep minima in the visual light curve. The extended dust shell (radius $\sim$ 19 mas) was first resolved by speckle interferometric observations with the SAO 6 m telescope (Ohnaka et al. 2001).

In the V and L light curves probably a ~4-year wind travel time from the stellar surface to the extended dust shell with a radius of approximately 110 stellar radii can be seen. The comparison of the V and L light curves shows that the period 1994–1998 of an increased (and decreasing) L and M brightness started approximately 4 years after the end (in 1990) of a period with many deep minima in the visual light curve. This can be explained if we assume that during phases of increased stellar magnetic activity (see studies by Soker & Clayton 1999) there is a simultaneous increase of both (i) the supergiant wind and (ii) the rate of formation of dust clouds. If this assumption is true, the increased stellar wind period ended in 1990. The L band brightness increased until 1994. This can be explained by the increased stellar wind until 1990 and a wind travel time of 4 years from the stellar surface to the extended dust shell region. In the period 1994–1999 the L band brightness was decreasing because in this period only lower intensity stellar wind arrived, which was produced during the low-activity period 1990–1995. We believe that the variation of the stellar wind can be considered as an indirect argument in favor of active phenomena on the surface of R CrB.

Acknowledgements. Nazar Ikhsanov acknowledges the support of the Alexander von Humboldt Foundation within the Long-term Cooperation Program. This research was partly supported by Russian Foundation for Basic Research (project No. 02-02-16235).

References

Asplund, M., Gustafsson, B., Kiselman, D., & Eriksson, K. 1997, A&A, 318, 521
Asplund, M., Gustafsson, B., & Lambert, D. A. 2000, A&A, 353, 287
Clayton, G. C. 1996, PASP, 108, 225
Colangeli, L., Mennella, V., Palumbo, P., et al. 1995, A&AS, 113, 561
Egan, M. P., Leung, C. M., & Spagna, G. F. 1988, Comput. Phys. Comm., 48, 271
Fadeyev, Yu. A. 1988, MNRAS, 233, 65
Feast, M. W., Carter, B. S., Roberts, G., et al. 1997, MNRAS, 285, 317
Feast, M. W. 1997, MNRAS, 285, 339
Fernie, J. D., & Seager, S. 1994, PASP, 106, 1138
Fernie, J. D. 1982, PASP, 94, 172
Fernie, J. D., Percy, J. R., & Richer, G. 1986, PASP, 98, 605
Forrest, W. J., Gillett, F. C., & Stein, W. A. 1972, ApJ, 178, L129
Genet, R. M., Boyd, L. J., Kissell, K. E., et al. 1987, PASP, 99, 660
Gillett, F. C., Backman, D. E., Beichman, C., & Neugebauer, G. 1986, ApJ, 310, 842
Jäger, C., Mutschke, H., & Henning, T. 1998, A&A, 332, 291
Jurcsik, J. 1996, Acta Astron., 46, 325
Leung, C. M. 1976, ApJ, 209, 75
Nadjip, A. E., Shenavrin, V. I., & Tikhonov, V. G. 1986, Trydy Gos. Astron. Inst. Sternberg, 58, 119
Ohnaka, K., Balega, Y., Blöcker, T., et al. 2001, A&A, 380, 212
Rao, N. K., & Nandy, K. 1986, MNRAS, 222, 357
Rao, N. K., Lambert, D. L., Adams, M. T., et al. 1999, MNRAS, 310, 717
Reimers, D. 1975, in Problems in Stellar Atmospheres and Envelopes, ed. B. Baschek, W. H. Kegel, & G. Traving (Springer, Berlin), 229
Rosenbush, A. E. 2001, IBVS, 5025
Shenavrin, V. I., Taranova, O. G., Moroz, V. I., & Grigor'ev, A. V. 1979, AZh, 56, 1007
Soker, N., & Clayton, G. C. 1999, MNRAS, 307, 993
Stein, W. A., Gaustad, J. E., Gillett, F. C., & Knacke, R. F. 1969, ApJ, 155, L3
Strecker, D. W. 1975, AJ, 80, 451
Yudin, B., Balega, Y., Blöcker, T., et al. 2001, A&A, 379, 229